IET Research Journals

Submission Template for IET Research Journal Papers

IET Journals
The Institution of Engineering and Technology

ISSN 1751-8644
doi: 0000000000
www.ietdl.org

A Multi-carrier Chaotic Communication Scheme for Underwater Acoustic Communications

Menglei Chen, Weikai Xu, Deqing Wang, Lin Wang*

*School of information science and engineering, Xiamen University, 361005 Xiamen, China * E-mail: xweikai@xmu.edu.cn*

Abstract: Multi-carrier (MC) and spread-spectrum (SS) are two good technologies for underwater acoustic (UWA) communications. In this paper, we propose a novel multi-carrier chaos modulation scheme, which combines code-shifted differential chaos shift keying (CS-DCSK) with orthogonal frequency division multiplexing (OFDM), namely MC-CS-DCSK. The proposed scheme exploits the orthogonal characteristic of the Walsh code to superimpose the chaotic reference chips and the information bearing chips in the same time/frequency unit. Besides, a cyclic-shift interleaver is used on chips to harvest frequency diversity. To the in-depth understanding of the proposed system, the bit error rate (BER) of the proposed system under Gaussian channels and multipath Rayleigh fading channels are derived and verified by simulation. Further, the spectral efficiency of the proposed system is analyzed and compared with some existing chaos-based communication systems. Finally, we study BER performance of the system under UWA channels and compare it with traditional multi-carrier direct sequence spread-spectrum (MC-DSSS) and OFDM-based multi-carrier DCSK systems. Simulation results show that the system has good robustness under time-varying UWA channels.

1 Introduction

Underwater acoustic (UWA) communications have attracted considerable attention over the last few decades due to the special economic and military strategic value of oceans which involves the interests and developments of various countries [1–3]. However, an UWA channel is a typical harsh and complex environment for information transmission. The performance of UWA communications is affected significantly by low propagation speed, large propagation delays, variations of the channel impulse response and so on [4]. The multipath transmission combined with lager propagation delays of UWA channels causes serious inter-symbol-interference (ISI) which may influence dozens of symbols. Variations of the channel impulse response results in severe Doppler spread [5].

Orthogonal frequency division multiplexing (OFDM) and direct sequence spread-spectrum (DSSS) are two good candidates to deal with the above problems. The OFDM with cyclic prefix works well on multipath propagation channels, because each sub-carrier can be treated as a narrowband transmission channel [6–8]. However, it is easy to induce inter-carrier interference (ICI) when the channel is time-varying [9]. Spread-spectrum communication system can provide a capacity of multi-access communication and mitigating multipath interference [10]. Moreover, SS has good communication security and high robustness to multipath interference. It is also a good choice for UWA communications. The combination of multi-carrier modulation and DSSS, namely multi-carrier (MC-DSSS), is an attempt to take advantage of attributes of both techniques [11–14]. Thus, it is also a promising scheme for underwater acoustic communications. In MC-DSSS [11], a PN sequence is firstly used to spread the bits. Then the chips of spread sequence are loaded onto different orthogonal sub-carriers. At the receiver, the received signals are demodulated by the correlators and maximal ratio combiners (MRC). However, MRC requests the estimation of the fading coefficients of each carrier, which increases the complexity of the receiver. In [12], a blind adaptive algorithm is presented. This algorithm can maximize the signal-to-noise ratio (SNR) by using a weight vector, which is better than MRC generally. Based on minimum mean square error (MMSE) filtering, adaptive equalizers and carrier phase estimators are applied [13]. Relative to OFDM and SS, MC-DSSS can achieve better performance over time-varying frequency selective channels. The above underwater acoustic communication systems usually employ advanced signal processing algorithms, such as complicated adaptive equalization or Rake receivers. The performances of these receivers are sensitive to the parameter choices of adaptive equalizers. The optimum parameters of these receivers vary a great deal according to different channel conditions. Therefore, it is essential to design a reliable and flexible communication scheme with low complexity and high data-rate for UWA communications.

The differential chaos shift keying (DCSK) can be regarded as a non-coherent spread spectrum system where the chaotic sequence is used as the spread sequence [15–17]. This system not only has the good performance over multipath fading channels, but also has a simple transceiver structure, i. e., without chaotic synchronization, channel estimation, and channel equalization. However, the defect of DCSK is that it has low energy efficiency and data rate as half of the chaos chips are used to transmit a reference signal [16]. Furthermore, radio frequency (RF) delay lines are required at the receiver because the reference signal and the information signal are transmitted in two slots, respectively. Thus, many schemes have been proposed to solve the mentioned problems. The proposed systems [18, 19] aim to increase the data rate which is realized by transmitting two orthogonal signals formed by a Hilbert transform. In [20], code shifted differential chaos shift keying (CS-DCSK) is proposed. It avoids RF delay lines at the receiver and has good performance in time-varying channels. To enhance data throughput, many multi-carrier DCSK systems are proposed [21–24]. The system in [21] is an OFDM-based multiuser chaos shift keying (MU OFDM-DCSK) modulation system. In this system, the reference signals of all users are inserted into predefined subcarriers with a comb-type insertion. Then the remained subcarriers are used to transmit information bearing signals of all users. In [22], a multi-carrier DCSK communication (MC-DCSK) system is presented. In this system, the reference signal is put in one predefined subcarrier and the information bearing signals are loaded on the rest of the subcarriers. The system in [23] is an M-ary multi-carrier DCSK(MM-DCSK) system. The system loads one non-information-bearing reference signal on the first subcarrier. Then the rest of the information bearing signals are all modulated based on their previous subcarrier. In [24], the authors proposed a multi-carrier chaos shift keying (MC-CSK) system. In the system, the reference signal and information bearing signals are transmitted

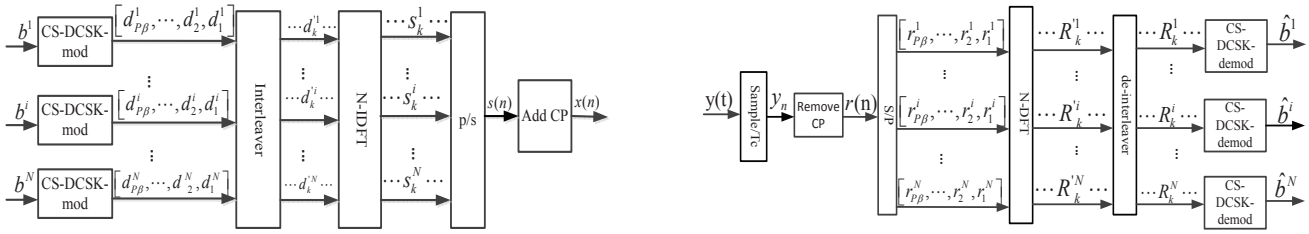

(a) Transmitter (b) Receiver

Fig. 1: Block diagram of MC-CS-DCSK system.

on the same subcarrier through I/Q components simultaneously. All above schemes, the reference signal and information bearing signals are loaded on different sub-carriers, respectively. Thus, they can not work well if they are applied to a severe frequency-selective fading channel where the channel impulse responses of the subcarriers are very different.

Motivations and Contributions: To overcome the weakness of the above multicarrier DCSK system, we proposed a multi-carrier DCSK based on CS-DCSK for doubly selective fading channel [25]. The system superimposes the reference signal and the information bearing signal in the same time/frequency unit. In this system, all chips of a CS-DCSK symbol are loaded on different subcarriers, respectively. Although this system demonstrated excellent performance over time/frequency selective fading channels, its spectral efficiency is decided by the number of sub-carriers since all chips of a CS-DCSK symbol are loaded on subcarriers of an OFDM symbol, i.e., the spreading factor should be the same as the number of the subcarriers. Besides, when the number of subcarriers is increased (The spreading factor is also increased.), the noise interference at the receiver will be aggravated.

In this paper, we proposed a novel OFDM-based multi-carrier CS-DCSK (MC-CS-DCSK) system. This system also incorporates CS-DCSK and OFDM. However, different from the system presented in [25], the number of subcarriers of the system is independent of the spreading factor, which brings more flexibility to the system to enable higher spectral efficiency.

The main contributions of this paper are listed as follows.

• We propose an OFDM-based multi-carrier DCSK system, i.e., MC-CS-DCSK. In the proposed system, N parallel reference signals and information bearing signals formed N CS-DCSK symbols by using Walsh code sequences. Then the chips of N CS-DCSK symbols are loaded on N subcarriers by inverse discrete Fourier transform (IDFT), respectively. Meantime, a cyclic-shift interleaver is used for every OFDM symbol to harvest frequency diversity. With the character of CS-DCSK, the reference signal and the information bearing signal are superimposed at the same time/frequency domain. Hence, the proposed system is robust over time-varying fading channels. By the use of OFDM, the proposed system has enhanced the capacity to resist the large delay spread of the channel.

• We derive the BER expressions of the proposed MC-CS-DCSK system under Gaussian and multipath Rayleigh fading channels. The analytical results are verified by simulations. The proposed system exhibits better BER performance over MC-DSSS, MM-DCSK [23], and OFDM-CS-DCSK [25] over UWA channels. We also analyze the spectral efficiency of the system and compare it with MM-DCSK and OFDM-CS-DCSK.

The remainder of the paper is organized as follows. In Section 2, the MC-CS-DCSK system model is presented. The analytical BER expression is derived and the spectral efficiency is given in Section 3. Section 4 demonstrates the numerical results and discussions. Conclusions are drawn in Section 5.

2 System Model

The proposed MC-CS-DCSK system is described in Fig.1(a). In this system, N parallel bits go into N CS-DCSK modulators, respectively, in which the bits are modulated by the CS-DCSK modulators. For each CS-DCSK modulator, $P\beta$ chips which form a CS-DCSK symbol are obtained for each bit by CS-DCSK modulation. Then, the chips from N CS-DCSK symbols are cyclic-shifted by an interleaver. For example, the first chips from the N CS-DCSK modulators form an N-length chip sequence. A random cyclic-shifter interleaves this N-length chip sequence. Then, the N-length interleaved chips are loaded onto mutually orthogonal sub-carriers by an inverse discrete Fourier transform (IDFT). The same operation is performed for the remaining chips of all CS-DCSK symbols.

The block diagram of a CS-DCSK modulator is described in Fig.2(a). A chaotic signal generator produces β chaos chips by a logistic map $c_{i+1} = 1 - 2c_i^2, i \in N^+$. Then the reference signal and information bearing signal of CS-DCSK are formed by the use of orthogonality of Walsh codes. We denote $\mathbf{W} = \left[\mathbf{w}_1{}^{\mathrm{T}}, \mathbf{w}_2{}^{\mathrm{T}}, \cdots, \mathbf{w}_P{}^{\mathrm{T}}\right]^{\mathrm{T}}$ a $P \times P$ Walsh code matrix, where $\mathbf{w}_i = [w_{i,1}, w_{i,2}, \cdots, w_{i.P}], 1 \le i \le P$. The β-length chaos chips are multiplied by each element of a specified $\mathbf{w}_R, R \in [1, P/2]$ to generate a reference signal which is comprised of $P\beta$ chips. The information bearing signal of CS-DCSK is also constructed by β-length chaos chips, another Walsh code $\mathbf{w}_I$ $(I \in [P/2, P])$ and information symbol a. The length of the information bearing signal is also $P\beta$. Finally, the reference signal is added with information bearing signal as the result of CS-DCSK modulation which is denoted $\mathbf{d}^l = [d^l_{P\beta-1}, \cdots, d^l_1, d^l_0], 1 \le l \le N$. $P\beta$ is the spreading factor of CS-DCSK. Thus, the modulated signal of the l^{th} CS-DCSK can be represented by

$$\mathbf{d}^l = \mathbf{w_R} \otimes \mathbf{c} + a_l \mathbf{w_I} \otimes \mathbf{c}, l = 1, 2..., N, \tag{1}$$

where $\mathbf{c} = \begin{bmatrix} c_1 & c_2 & \cdots & c_\beta \end{bmatrix}$ is a chaotic sequence consisting of β chaotic chips, $a_l \in \{-1, +1\}$ mapped from $b^l \in \{0, 1\}$ is the information symbol modulated by the l^{th} CS-DCSK modulator, $\mathbf{w}_R = [w_{R,1}, w_{R,2}, \cdots, w_{R,P}]$ and $\mathbf{w}_I = [w_{I,1}, w_{I,2}, \cdots, w_{I,P}]$ are two rows of Walsh code matrix used for constructing the reference signal and the information bearing signal, respectively, $\otimes$ is the Kronecker operator.

The N parallel CS-DCSK signals is expressed as

$$\mathbf{T} = \begin{bmatrix} d_0^1 & d_1^1 & \cdots & d_{P\beta-1}^1 \\ d_0^2 & d_1^2 & \cdots & d_{P\beta-1}^2 \\ \vdots & \vdots & \ddots & \vdots \\ d_0^N & d_1^N & \cdots & d_{P\beta-1}^N \end{bmatrix}, \tag{2}$$

where $\mathbf{d}^i = \begin{bmatrix} d_0^i & d_1^i & \cdots & d_{P\beta-1}^i \end{bmatrix}, i \in [1, N]$ means the i^{th} CS-DCSK signal. Let $\mathbf{Y}_k = [d_k^1, d_k^2, \cdots, d_k^N]^T, k = 0, 1, \cdots, P\beta - 1$ means the k^{th} OFDM symbol. The vector $\mathbf{Y}_k^{'} = \mathbf{Q}^j \mathbf{Y}_k = \begin{bmatrix} d_k^{'1} & d_k^{'2} & \cdots & d_k^{'N} \end{bmatrix}$ is the form of an original spreading sequence $\mathbf{Y}_k$ circularly shifted by j chips, here $\mathbf{Q}^j$ is power of matrix $\mathbf{Q}$. The circular shift matrix $\mathbf{Q}$ is defined as

$$\mathbf{Q} := \begin{bmatrix} 0_{1\times(N-1)} & 1 \\ \mathbf{I}_{N-1} & 0_{(N-1)\times 1} \end{bmatrix}, \tag{3}$$

where $\mathbf{I}_N$ is a $N \times N$ identity matrix.

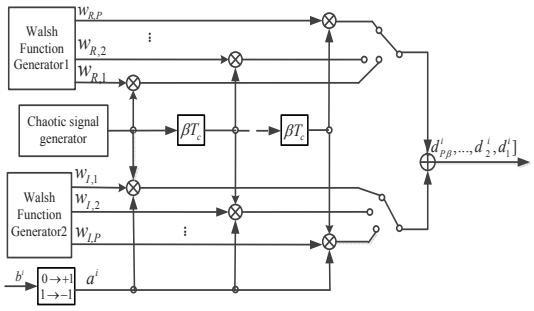

(a) Transmitter

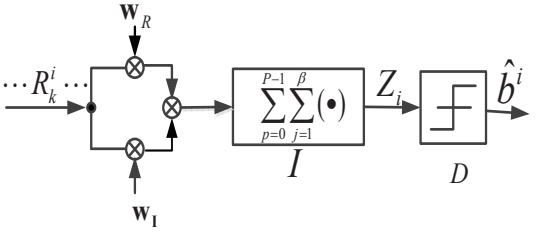

(b) Receiver

Fig. 2: Block diagram of CS-DCSK tranceiver.

Finally, chips of the k^{th} OFDM symbol $\mathbf{Y}_k^{'}, k \in [0, P\beta - 1]$ is loaded on N different subcarriers by IDFT. The signal structure of an MC-CS-DCSK symbol is shown in Fig.3. Therefore, the transmitted signal is written as

$$s(t) = \sum_{k=1}^{P\beta} \sum_{i=1}^{N} \left\{ d_k^{'i} \cos\left[2\pi \left(f_c + i\Delta f\right) t + \varphi_i\right] \mathrm{rect}(t - kT_s) \right\}, \tag{4}$$

where Δf is bandwidth of sub-carrier, T_s is duration of the OFDM symbol, f_c is carrier frequency, φ_i is the random phase of the i^{th} sub-carrier, N is the number of sub-carriers, and $\mathrm{rect}(t - kT_s)$ is the pulse waveform, which is defined as

$$\mathrm{rect}(t - kT_s) = \begin{cases} 1, & t \in [(k-1)T_s, kT_s] \\ 0, & \text{otherwise} \end{cases}. \tag{5}$$

The receiver structure of MC-CS-DCSK system is illustrated in Fig.1(b). The received signal $y(t)$ is sampled with time interval $T_c = T_s/N$. Next the cyclic prefix is removed to obtain a discrete signal $r(n)$. Then it is converted to parallel data by a serial-to-parallel converter. Thus, the $i^{\mathrm{th}}(1 \le i \le N)$ time-domain sample of $k^{\mathrm{th}}(1 \le k \le P\beta)$ OFDM symbol is expressed as

$$r_k^i = \sum_{l=0}^{L-1} h_{i,l}^k s_k((i-l))_N + \eta_{i,k}, \tag{6}$$

where $\eta_{i,k}$ is the complex Gaussian noise with zero mean and variance N_0, L denotes the number of paths of UWA channel, $((\bullet))_N$ represents a cyclic shift with the base of N, $h_{i,l}^k$ is the l^{th} channel response at time instant $t = [(k-1)N + i]\, T_c$ of time-varying UWA channel, which is

$$h(t, \tau) = \sum_{l=0}^{L-1} A_l(t)\delta(\tau - \tau_l(t)), \tag{7}$$

where $A_l(t)$ and $\tau_l(t)$ are the amplitude and delay of l^{th} channel tap, respectively.

Next, the N parallel signals are fed into the DFT processor to demodulate information chips for each sub-carrier.The chip on the $n^{\mathrm{th}}(1 \le n \le N)$ sub-carrier of the $k^{\mathrm{th}}(1 \le k \le P\beta)$ OFDM symbol is

$$R_n^{'k} = S_{k,n} H_{n,n}^k + \sum_{i=1, i\neq n}^{N} H_{n,i}^k S_{k,i} + N_{k,n}, \tag{8}$$

where $S_{k,i}$ is frequency domain form of $s_k(i)$, and $H_{n,d}^k$ is the frequency response of UWA channel which is

$$H_{n,d}^k = \frac{1}{N} \sum_{l=0}^{L-1} \sum_{m=1}^{N} h_{m,l}^k e^{\frac{-j2\pi(md + l(n-d))}{N}} \qquad 1 \le n, d \ \le N. \tag{9}$$

In the following, the signal is inversely cycle-shifted by the deinterleaver. The output of deinterleaver is expressed as

$$\mathbf{R}_k = (\mathbf{Q}^j)^T \mathbf{R}_k^{'}, 1 \le k \le P\beta, \tag{10}$$

where $\mathbf{R}_k^{'} = [R_k^{'1}, R_k^{'2}, \cdots, R_k^{'N}]^T$.

After de-interleaving, the signal is demodulated by a CS-DCSK demodulator, which is shown in Fig.2(b). According to the principle of the CS-DCSK demodulation, the decision variable of the $i^{\mathrm{th}}(1 \le i \le N)$ CS-DCSK receiver is

$$Z_i = \mathrm{Re}\left\{ \sum_{p=0}^{P-1} \left(w_{R,p+1} w_{I,p+1} \sum_{j=1}^{\beta} R_{p\beta+j}^i \left(R_{p\beta+j}^i \right)^* \right) \right\}, \tag{11}$$

where $\mathrm{Re}\,(x)$ means the real part of variable x, $(x)^*$ denotes the conjugate of x. The estimated bit $\hat{b}^i$ is obtained by

$$\hat{b}^i = \mathrm{sign}(Z_i), \tag{12}$$

where $\mathrm{sign}\,(\cdot)$ represents a decision function. It returns 1 if Z_i is greater than 0, otherwise returns 0.

3 Performance Analysis

3.1 BER Analysis of MC-CS-DCSK

In this section, the BER expressions of MC-CS-DCSK system under AWGN and multipath Rayleigh fading channels are derived. Assuming the impulse response of the multipath Rayleigh channel is

$$h\,(t) = \sum_{l=0}^{L-1} \alpha_l \delta\,(t - \tau_l), \tag{13}$$

where L is the number of paths, α_l is the channel coefficient of the l^{th} path, and τ_l is the time delay of the l^{th} path. The channel coefficient follows a Rayleigh distribution, its probability density function is

$$f\,(x) = \frac{x}{\sigma^2} e^{-\frac{x^2}{2\sigma^2}}, x > 0, \tag{14}$$

where $\sigma > 0$ is the scale parameter of the Rayleigh distribution.

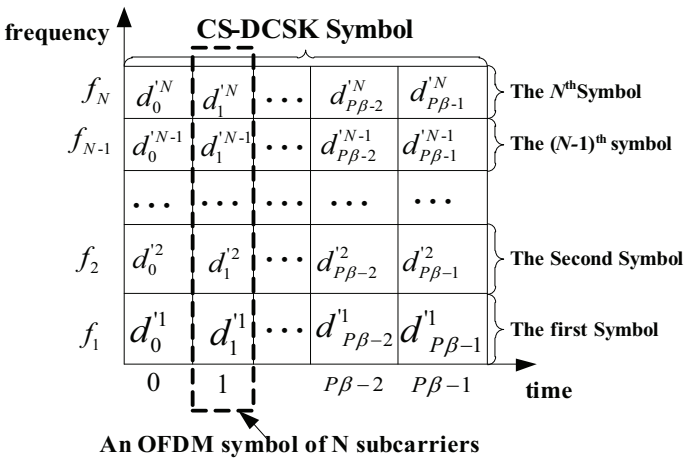

Fig. 3: MC-CS-DCSK signal structure.

In the multipath channel, the delay of paths will introduce inter-symbol interference (ISI). In this section, we assume that the maximum delay spread is far smaller than the length of a symbol, i.e. $0 \leq \tau_{l\max} << P\beta T_s$. This assumption holds in many references [26]. Under the assumption, ISI can be ignored. Since chaotic signals are sensitive to initialization, chaotic sequences with different initializations are independent. Besides, due to the properties of autocorrelation and cross-correlation of the chaotic sequences, for a larger spreading factor, we have $\sum_{k=1}^{\beta} c_{k-\tau_l} c_{k-\tau_j} \approx 0, l \neq j$ [27]. Finally, the chaotic sequences are also independent of the Gaussian noises [28].

For MC-CS-DCSK, the signal on every subcarrier has the same structure and we give the BER performance derivation of the signal on the $i^{th}(1 \leq i \leq N)$ subcarrier without loss of generality. The expression of the decision variable Z of the i^{th} bit is

$$\begin{aligned} Z &= \sum_{k=0}^{P-1}\left(w_{R,k+1}w_{I,k+1}\sum_{j=1}^{\beta}R_{k\beta+j}R_{k\beta+j}^{*}\right) \\ &= \sum_{k=0}^{P-1}\left[w_{R,k+1}w_{I,k+1}\sum_{j=1}^{\beta}\left(\sum_{l=1}^{L}\alpha_l S_{k\beta+j-\tau_l}+N_{k\beta+j}\right)\times\right. \\ &\left.\left(\sum_{l=1}^{L}\alpha_l S_{k\beta+j-\tau_l}+N_{k\beta+j}\right)^{*}\right], \end{aligned} \tag{15}$$

where $S_{k\beta+j-\tau_l} = \left(w_{R,k+1} + aw_{I,k+1}\right)c_{k\beta+j-\tau_l}$, α_l and τ_l are the channel coefficient and time delay of the l^{th} path respectively. $N_{k\beta+j}$ is a complex Gaussian noise and $N_{k\beta+j}^{*}$ denotes its conjugate. To derive the BER formula of the MC-CS-DCSK system, we need to calculate mean and variance of the observation signal Z. We separate Z into $Z = A + B + C$ in which A is the useful information whose expression is

$$\begin{aligned} A = \sum_{k=0}^{P-1} w_{R,k+1}w_{I,k+1}\sum_{j=1}^{\beta}\sum_{l=1}^{L}\alpha_l^2\left[\left(w_{R,k+1}+aw_{I,k+1}\right)\times\right. \\ \left.c_{k\beta+j-\tau_l}\right]^2. \end{aligned} \tag{16}$$

B and C are interferences parts with the following expression

$$\begin{aligned} B = \sum_{k=0}^{P-1} w_{R,k+1}w_{I,k+1}\sum_{j=1}^{\beta}\left[\sum_{l=1}^{L}\alpha_l\left(w_{R,k+1}\right.\right. \\ \left.\left.+aw_{I,k+1}\right)c_{k\beta+j-\tau_l}\left(N_{k\beta+j}{}^{*}+N_{k\beta+j}\right)\right], \end{aligned} \tag{17}$$

$$C = \sum_{k=0}^{P-1} w_{R,k+1}.w_{I,k+1}\sum_{j=1}^{\beta}\left|N_{k\beta+j}\right|^2. \tag{18}$$

When the transmitted symbol is $a = +1$, the mean and variance of above quantities can be calculated as

$$\mathrm{E}\left[\mathrm{A}|\mathrm{a}=+1\right] = 2\sum_{\mathrm{l}=1}^{\mathrm{L}}\alpha_{\mathrm{l}}^2\mathrm{P}\beta\mathrm{E}\left[\mathrm{c}_{\mathrm{j}}^2\right], \tag{19}$$

$$\mathrm{E}\left[\mathrm{B}|\mathrm{a}=+1\right] = \mathrm{E}\left[\mathrm{C}|\mathrm{a}=+1\right] = 0, \tag{20}$$

$$\begin{aligned} &\mathrm{Var}[\mathrm{A}|\mathrm{a}=+1] = \mathrm{E}\left[\mathrm{A}^2|\mathrm{a}=+1\right] - \mathrm{E}^2\left[\mathrm{A}|\mathrm{a}=+1\right] \\ &= 8\left(\sum_{l=1}^{L}\alpha_l^2\right)^2 P\beta\mathrm{Var}\left[c_j^2\right], \end{aligned} \tag{21}$$

$$\begin{aligned} &\mathrm{Var}\left[\mathrm{B}|\mathrm{a}=+1\right] = \mathrm{E}\left[\mathrm{B}^2|\mathrm{a}=+1\right] - \mathrm{E}^2\left[\mathrm{B}|\mathrm{a}=+1\right] \\ &= 4\sum_{l=1}^{L}\alpha_l^2 P\beta N_0\mathrm{E}\left[\mathrm{c}_{\mathrm{j}}^2\right], \end{aligned} \tag{22}$$

$$\mathrm{Var}\left[\mathrm{C}|\mathrm{a}=+1\right] = \mathrm{P}\beta\mathrm{Var}\left[\left|\mathrm{N}_{\mathrm{k}\beta+\mathrm{j}}\right|^2\right] = \mathrm{P}\beta\mathrm{N}_0^2. \tag{23}$$

Thus, the mean of Z is

$$\mathrm{E}\left[\mathrm{Z}|\mathrm{a}=+1\right] = 2\sum_{\mathrm{l}=1}^{\mathrm{L}}\alpha_{\mathrm{l}}^2\mathrm{P}\beta\mathrm{E}\left[\mathrm{c}_{\mathrm{j}}^2\right]. \tag{24}$$

Since A, B, and C are independent, the covariance is zero for any two of them. Therefore, the variance of Z can be written as

$$\begin{aligned} &\mathrm{Var}\left[\mathrm{Z}|\mathrm{a}=+1\right] = 8\left(\sum_{\mathrm{l}=1}^{\mathrm{L}}\alpha_{\mathrm{l}}^2\right)^2\mathrm{P}\beta\mathrm{Var}\left[\mathrm{c}_{\mathrm{j}}^2\right] \\ &+8\sum_{l=1}^{L}\alpha_l^2 P\beta N_0\mathrm{E}\left[\mathrm{c}_{\mathrm{j}}^2\right] + \mathrm{P}\beta\mathrm{N}_0^2. \end{aligned} \tag{25}$$

When the transmitted symbol is $a = -1$, the mean and variance of Z can be expressed as

$$\mathrm{E}\left[\mathrm{Z}|\mathrm{a}=-1\right] = -\mathrm{E}\left[\mathrm{Z}|\mathrm{a}=+1\right], \tag{26}$$

$$\mathrm{Var}\left[\mathrm{Z}|\mathrm{a}=-1\right] = \mathrm{Var}\left[\mathrm{Z}|\mathrm{a}=+1\right]. \tag{27}$$

The transmitted bit energy $E_b = 2P\beta\mathrm{E}\left[\mathrm{c}_{\mathrm{j}}^2\right]$ can be assumed to be constant when spreading factor is large. And we know that Z follows a Gaussian distribution. By central limit theorem, the BER can be written as

$$\begin{aligned} BER &= \tfrac{1}{2}\Pr\left(Z<0|a=+1\right) + \tfrac{1}{2}\Pr\left(Z\geq 0|a=-1\right) \\ &= \tfrac{1}{2}\mathrm{erfc}\left(\frac{\mathrm{E}\{\mathrm{Z}|\mathrm{a}=+1\}}{\sqrt{2\mathrm{Var}\{\mathrm{Z}|\mathrm{a}=+1\}}}\right) \\ &= \tfrac{1}{2}\mathrm{erfc}\left(\frac{2\sum_{\mathrm{l}=1}^{\mathrm{L}}\alpha_{\mathrm{l}}^2\mathrm{P}\beta\mathrm{E}[\mathrm{c}_{\mathrm{j}}^2]}{\sqrt{2(8\mathrm{P}\beta\left(\sum_{\mathrm{l}=1}^{\mathrm{L}}\alpha_{\mathrm{l}}^2\right)^2\mathrm{Var}\left[\mathrm{c}_{\mathrm{j}}^2\right]+4\sum_{\mathrm{l}=1}^{\mathrm{L}}\alpha_{\mathrm{l}}^2\mathrm{P}\beta\mathrm{N}_0\mathrm{E}\left[\mathrm{c}_{\mathrm{j}}^2\right]+\mathrm{P}\beta\mathrm{N}_0^2)}}\right) \\ &= \tfrac{1}{2}\mathrm{erfc}\left(\left(\frac{4\mathrm{Var}\left[\mathrm{c}_{\mathrm{j}}^2\right]}{\mathrm{P}\beta\mathrm{E}^2\left[\mathrm{c}_{\mathrm{j}}^2\right]}+\frac{4\mathrm{N}_0}{\sum_{\mathrm{l}=1}^{\mathrm{L}}\alpha_{\mathrm{l}}^2\mathrm{E}_{\mathrm{b}}}+\frac{2\mathrm{P}\beta{\mathrm{N}_0}^2}{\left(\sum_{\mathrm{l}=1}^{\mathrm{L}}\alpha_{\mathrm{l}}^2\mathrm{E}_{\mathrm{b}}\right)^2}\right)^{-\frac{1}{2}}\right), \end{aligned} \tag{28}$$

where $\mathrm{erfc}\left(\cdot\right)$ is the complementary error function defined by $\mathrm{erfc}\left(\mathrm{x}\right) = \left(2/\sqrt{\pi}\right)\int_{\mathrm{x}}^{+\infty}\mathrm{e}^{-\mu^2}\mathrm{d}\mu$, the mean and variance of the energy of chaos chips are equal to $1/2$ and $1/8$ respectively, i.e. $\mathrm{E}\left[\mathrm{c}_{\mathrm{j}}^2\right] = 1/2$, $\mathrm{Var}\left[\mathrm{c}_{\mathrm{j}}^2\right] = 1/8$.

We define $\gamma_b = \sum_{l=1}^{L} \alpha_l^2 E_b/N_0$ as instantaneous SNR. The BER expression of the proposed system can be rewritten as

$$BER = \frac{1}{2}\mathrm{erfc}\left\{\left(\frac{2}{\mathrm{P}\beta} + \frac{4}{\gamma_\mathrm{b}} + \frac{2\mathrm{P}\beta}{\gamma_\mathrm{b}^2}\right)^{-\frac{1}{2}}\right\}. \quad (29)$$

For i.i.d. Rayleigh fading channels, the PDF of instantaneous SNR γ_b is

$$f(\gamma_b) = \frac{1}{\bar{\gamma}_c^{\mathrm{L}}(L-1)!}\gamma_b^{L-1} e^{-\frac{\gamma_b}{\bar{\gamma}_c}}, \quad (30)$$

where $\bar{\gamma}_c$ is the average SNR of every path with expression $\bar{\gamma}_c = E\left(\alpha_l^2\right)(E_b/N_0) = E\left(\alpha_j^2\right)(E_b/N_0), j \neq l$.

For dissimilar Rayleigh fading channels, the PDF of γ_b is

$$f(\gamma_b) = \sum_{l=0}^{L-1} \frac{\pi_l}{\bar{\gamma}_l} e^{-\frac{\gamma_b}{\bar{\gamma}_l}}, \quad (31)$$

where $\pi_l = \prod_{j=0, j\neq l}^{L-1} \frac{\bar{\gamma}_l}{\bar{\gamma}_l - \bar{\gamma}_j}$, and $\bar{\gamma}_l$ is the average value of the l^{th} path instantaneous SNR $\gamma_l = \alpha_l^2 (E_b/N_0)$.

In conclusion, the BER of MC-CS-DCSK system can be expressed as

$$\begin{aligned} BER &= \int_0^{+\infty} BER(\gamma_b) f(\gamma_b)\, \mathrm{d}\gamma_\mathrm{b} \\ &= \int_0^{+\infty} \frac{1}{2}\mathrm{erfc}\left\{\left(\frac{2}{\mathrm{P}\beta} + \frac{4}{\gamma_\mathrm{b}} + \frac{2\mathrm{P}\beta}{\gamma_\mathrm{b}^2}\right)^{-\frac{1}{2}}\right\} \mathrm{f}(\gamma_\mathrm{b})\, \mathrm{d}\gamma_\mathrm{b}. \end{aligned} \quad (32)$$

In addition, in AWGN channels, the received signal is only corrupted by a complex additive Gaussian white noise with zero-mean and variance N_0. Thus, the number of paths $L = 1$, channel coefficient α=1, the instantaneous SNR γ_b=E_b/N_0. For high spreading factor, the bit energy $E_b = 2P\beta \mathrm{E}\left[\mathrm{c_j^2}\right]$ can be considered as a constant and the BER is

$$BER = \frac{1}{2}\mathrm{erfc}\left\{\left(\frac{2}{\mathrm{P}\beta} + \frac{4}{(\mathrm{E_b/N_0})} + \frac{2\mathrm{P}\beta}{(\mathrm{E_b/N_0})^2}\right)^{-\frac{1}{2}}\right\}. \quad (33)$$

3.2 Spectral Efficiency

In this section, we analyze the spectral efficiency of the MC-CS-DCSK system and compare it with MM-DCSK[23], and OFDM-CS-DCSK[25]. Spectral efficiency is defined as the bit rate (BR) in unit bandwidth (BW), i.e. the ratio between bit rate and bandwidth. Denote B as the system bandwidth, β as the length of the chaotic sequence, SF as the spreading factor, N as the number of subcarriers.

For multicarrier systems based on OFDM, the subcarriers can overlap with each other and we have the following relationship between the number of subcarriers and system bandwidth

$$B = N\Delta f = \frac{N}{T_s}, \quad (34)$$

where $T_s = 1/\Delta f$ is the duration of a symbol, Δf is the bandwidth of subcarrier, and N is the number of subcarriers.

MM-DCSK transmits a reference signal in the first subcarrier, and transmits the information bearing signals in the following $N-1$ subcarriers. Thus, the bit rate of this system is $BR_{MM-DCSK} = (N-1)/(SFT_s)$, where $T_s = N/B$, $SF = \beta$, and its spectral efficiency is

$$\begin{aligned} SE_{MM-DCSK} &= \frac{BR_{MM-DCSK}}{BW_{MM-DCSK}} = \frac{(N-1)/(SFT_s)}{B} \\ &= \frac{(N-1)/(SFT_s)}{N/T_s} = \frac{N-1}{SFN}. \end{aligned} \quad (35)$$

For OFDM-CS-DCSK system, assum the length of chaotic sequence is β, its spreading factor is $P\beta$. The systems load $P\beta$ chips of a CS-DCSK symbol on $P\beta$ different subcarriers, i. e., the number of subcarriers equals to the spreading factor. Therefore, the time required for transmitting a symbol is $T_s = N/B$=SF/B, here $SF = P\beta$, P is the length of Walsh code sequence. The spectral efficiency of this system is

$$\begin{aligned} SE_{OFDM-CS-DCSK} &= \frac{BR_{OFDM-CS-DCSK}}{BW_{OFDM-CS-DCSK}} = \frac{1/(T_s)}{B} \\ &= \frac{1/(T_s)}{P\beta/T_s} = \frac{1}{N}. \end{aligned} \quad (36)$$

MC-CS-DCSK is similar to OFDM-CS-DCSK, the information bearing signal is added with the reference signal in the time domain and its spreading factor is also $SF = P\beta$. However, the system transmits a CS-DCSK signal with each subcarrier and N CS-DCSK signals are transmitted with N subcarriers. The duration of each bit is SFT_s and $T_s = N/B$. Thus, its bit rate is

$$BR_{MC-CS-DCSK} = \frac{N}{SFT_s}, \quad (37)$$

and its spectral efficiency is

$$\begin{aligned} SE_{MC-CS-DCSK} &= \frac{BR_{MC-CS-DCSK}}{BW_{MC-CS-DCSK}} = \frac{N/(P\beta T_s)}{B} \\ &= \frac{N/(P\beta T_s)}{N/T_s} = \frac{N}{P\beta N} = \frac{1}{SF}. \end{aligned} \quad (38)$$

From the above results, we can see that MM-DCSK does not transmit any information on the first subcarrier, thus its spectral efficiency is lower than MC-CS-DCSK. Compared with OFDM-CS-DCSK, the number of subcarriers in MC-CS-DCSK is independent of its spreading factor, which adds more flexibility of the system. We can see that when $N = SF$, the spectral efficiency of MC-CS-DCSK is the same as OFDM-CS-DCSK but when $N > SF$, the spectral efficiency of MC-CS-DCSK is higher than OFDM-CS-DCSK. Since both N and SF are parameters to be set by the user, one may wonder if we can tune N in OFDM-CS-DCSK to match the spectral efficiency of MC-CS-DCSK. This is a bad idea in some scenarios. For example, for UWA channels with large delay spread, the number of subcarriers cannot be too small because it will deteriorate the BER performance significantly, which can be seen in Fig.7(a) in Section 4.

4 Numerical Results and Discussion

In this section, we first verify the derived BER expressions of MC-CS-DCSK over AWGN and multipath fading channels. Then, we investigate the performance of the proposed system over three time-varying UWA channels, the first one has a large delay spread, the remaining two have less delay spread. In addition, we also give the PAPR performance of the MC-CS-DCSK system.

In all figures, CP represents the length of cyclic prefix, SF means the spreading factor, N is the number of sub-carriers, T_s is the duration of a multiple carrier symbol, and L is the number of paths. The PAPR performance is evaluated in terms of the complementary cumulative distribution function (CCDF) [30], which is defined as $\mathrm{CCDF}(PAPR_0) = \Pr(PAPR > PAPR_0)$.

To make the simulation more convincing, the underwater acoustic channel simulation model in [31] is used. Simulation results are obtained from 1500 channel impulse responses with a time-varying convolution [3]. In this paper, three channel scenarios are investigated. They are denoted by Channel-I, Channel-II, and Channel-III, respectively. In the simulation, the system bandwidth is set to be the same as the bandwidth of the simulated channel, and the channel impulse response (CIR) is power-normalized. Simulation parameters for three channels are summarized in Table I. The geometry structure and delay-power spectrum of Channel-I, Channel-II and Channel-III are shown in Fig.4.

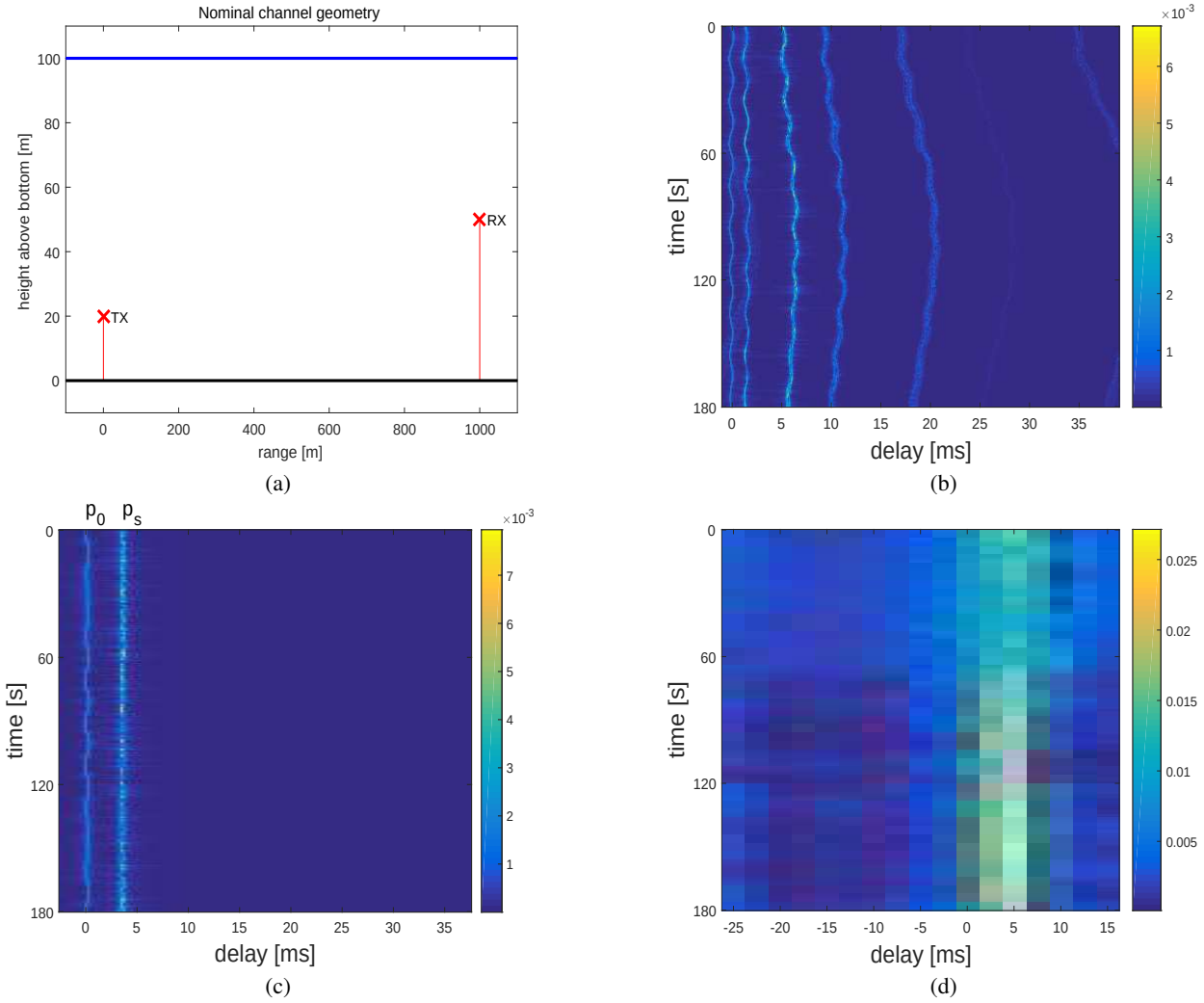

Fig. 4: Time-varying UWA channels. (a) The geometry of transmitter/receiver in three UWA channels. (b) Channel impulse response evolution over 180s duration of Channel-I. (c) Channel impulse response evolution over 180s duration of Channel-II. (b) Channel impulse response evolution over 180s duration of Channel-III.

Table 1 Main acoustic and geometric parameters of three UWA channels

Depth of transmitter	20m
Depth of receiver	50m
Horizontal distance	1000m
The speed of sound in water	1500m/s
The speed of sound on the sea floor	1200m/s
Bottom depth	100m
Center frequency(kHz) (Channel-I)	15
Bandwidth(kHz) (Channel-I)	10
Center frequency (kHz)(Channel-II)	15
Bandwidth(kHz) (Channel-II)	4
Center frequency (kHz)(Channel-III)	1.5
Bandwidth(Hz) (Channel-III)	400

4.1 Verification of the BER expressions and evaluation of the BER performance over AWGN and multipath Rayleigh fading channels

Figure 5 shows the simulated and analytical results of the MC-CS-DCSK system. The parameters are $SF = [64, 128, 256]$, $N = [64, 128]$, $CP = T_s/8$. From the figure, we can see that the simulated curves for the different number of subcarriers are overlapped with the same spreading factor. This is because the performance of the system is independent of the number of subcarriers, i. e., the number of subcarriers is absent in equation (32). Moreover, the agreement between simulated curves and the theoretical ones validates the correctness of our theoretical derivations. Besides, it can be seen that the performance of the system decreases with the increasing of the spreading factor. This is because the spreading gain is less than the noise interference introduced by the increasing of spreading factor.

Figure 6 shows the analytical and simulated results of the MC-CS-DCSK system under multipath fading channels, where $SF = 32, N = 128, CP = T_s/8, L = 1, 3, 7$. From the figure, we also can see that the simulated curves coincide with the theoretical curves. Furthermore, the performance of the system improves as the increasing of the number of channel's paths. This is because the system harvests frequency diversity by introducing cyclic-shift interleaver.

4.2 Performance comparisons of the proposed systems with other similar systems over UWA channels

Figure 7 shows the BER performance and PAPR performance of MC-CS-DCSK and MC-DSSS over UWA Channel-I. The simulation parameters are set to $SF = 32, CP = T_s/8, N = [128, 256, 512, 1024]$. It can be seen from Fig.7(a) that the performances of both MC-CS-DCSK and MC-DSSS improve with the increasing of the number of sub-carrier N when N is small. Since the symbol duration of OFDM increases with N for the given system bandwidth, the effect of inter-symbol-interference (ISI) gradually

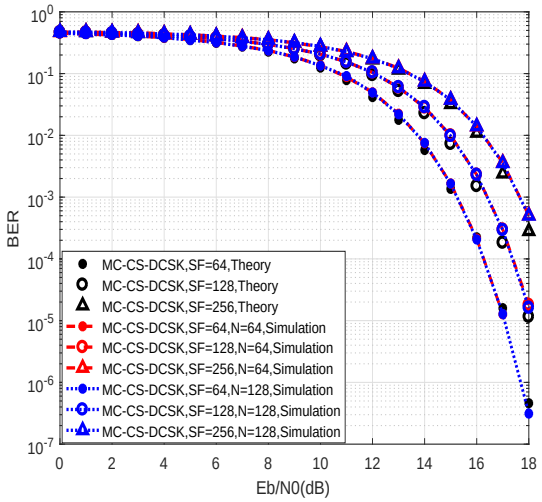

Fig. 5: Simulations and analytical BER performance of the MC-CS-DCSK system under an AWGN channel. The parameters $SF = [64, 128, 256]$, $N = [64, 128]$, $CP = T_s/8$.

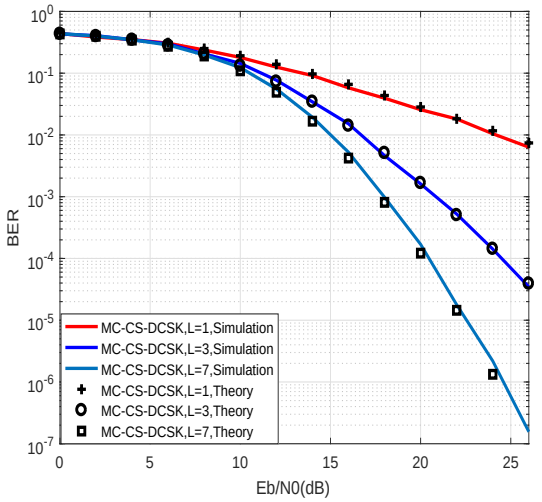

Fig. 6: Simulations and analytical BER performance of the MC-CS-DCSK system over multipath Rayleigh fading channels. The parameters are $SF = 32$, $N = 128$, $CP = T_s/8$, $L = 1, 3, 7$.

reduces. The performance of MC-CS-DCSK is significantly better than that of MC-DSSS with a small N. As N increases to a much larger value, MC-CS-DCSK behaves worse than MC-DSSS. However, the BER level of MC-CS-DCSK still reached to 10^{-5} when $SNR = 22$dB, which is completely acceptable in practical applications. As shown in Fig.7(b), the PAPR performance of both MC-CS-DCSK and MC-DSSS deteriorates with the increasing of N. However, the PAPR performance of MC-CS-DCSK is better than that of MC-DSSS. In addition, MC-DSSS is based on coherent modulation which requires channel estimation and equalization, while MC-CS-DCSK uses non-coherent detection and resultantly it has an obvious advantage in terms of complexity.

Figure 8(a) shows the BER performance of MC-CS-DCSK, OFDM-CS-DCSK, and MM-DCSK under the UWA channel-II, where $SF = 32$, $N = [64, 128, 256]$, $CP = T_s/8$. From the figure, one can observe that MC-CS-DCSK performs better than OFDM-CS-DCSK and MM-DCSK. For MC-CS-DCSK, its performance almost does not change when the number of subcarriers is increased from 128 to 256. This is because the maximum delay spread of UWA channel-II is about 4ms, whose coherent bandwidth is larger than the bandwidth of subcarriers for both $N = 128$ and $N = 256$. They have the same resilient ability to ISI. Thus, increasing the number of subcarriers from 128 to 256 will not change the performance much. For OFDM-CS-DCSK, the performance first improves as increasing the number of subcarriers from 64 to 128, then deteriorates as the number of subcarriers from 128 to 256. As increasing the number of subcarriers, the duration of the symbol will be enlarged, which results in a better ability to against ISI. However, since the number of subcarriers of OFDM-CS-DCSK equals to the spreading factor. Further increasing the number subcarrier, more noise will be introduced, which results in performance deterioration. For MM-DCSK, although its performance improves with the increasing of the number of subcarriers, its best performance is still worse than that of MC-CS-DCSK. This is because the reference signal and information bearing signals of the MM-DCSK system are transmitted on different subcarriers. The impulse responses of the reference subcarrier and the information bearing subcarriers will be different when time/frequency selective UWA channels are adopted. It makes the system show error floor at high SNR range.

Figure 8 (b) compares the BER performance of the systems over UWA channel-III. From the figure, we can see that MC-CS-DCSK achieves the best performance. OFDM-CS-DCSK system shows error floor when $N = 16$. BER can only reach the level of 10^{-4} at $SNR = 22dB$. For MM-DCSK system, error floor appears at $SNR = 16dB$ and BER can only reach the level of 10^{-2} for $N = 16, 32$. For MC-CS-DCSK, the system performs relatively good for $SNR = 20dB$ and $N = 16$. BER reaches the level of 10^{-6}. Since the UWA channel-III has relatively small maximum delay spread, the performance of MC-CS-DCSK does not further improve when the number of subcarriers is increased from 16 to 32. There is the same reason for the tendency shown in Figure 8(a).

4.3 *Effect of SF, CP, and interleaver*

Figure 9 shows the effect of the spreading factor on the BER performance of MC-CS-DCSK over the UWA channels. In Figure 9 (a), the BER performance of the proposed system with different spreading factors over the UWA channel-I are plotted for $SF = [8, 32, 64]$, $N = 512$, $CP = T_s/8$. It can be seen that the performance improves as the spreading factor increases from 8 to 32. However, the improvement is a bit for the increasing spreading factor from 32 to 64. Figure 9 (b) shows the performance of the system with different spreading factors over the UWA channel-III with parameters $SF = [8, 32, 64]$, $N = 16$, $CP = T_s/8$. In this channel, the performance improves as the increasing of spreading factor from 8 to 32 and deteriorates as the increasing of spreading factor from 32 to 64. This is similar to UWA channel-I. In conclusion, for MC-CS-DCSK, BER will improve with the increasing of the spreading a certain extent, but a too large spreading factor will undermine system performance. A proper spreading factor needs to be considered for a given transmission environment. For example, 32 will be a suitable spreading factor for UWA channel-I and UWA channel-III.

Figure 10 (a) illustrates the influence of the cyclic prefix on the performance of MC-CS-DCSK in UWA Channel-I. The simulation parameters are set as $SF = 32$, $CP = [0, T_s/8]$, $N = [128, 256, 512]$. One can observe that the BER performance of MC-CS-DCSK improves with the increasing of N. Besides, we can see that the BER performance of the system with CP is better than that of the system without CP. However, a sufficiently low BER level can be reached without CP when the number of sub-carriers is large enough. For example, $N = 512$, the BER can be reduced to 10^{-6} when $SNR = 26$dB. This is another good characteristic of the proposed system. We can abandon CP to further increase transmission efficiency in some transmission scenarios.

In Fig.10 (b), we investigate the effect of the interleaver on the performance of MC-CS-DCSK over UWA Channel-I. The simulation parameters are set as $SF = 32$, $CP = T_s/8$, $N = [128, 256, 512]$. It can be seen that the performance of the system

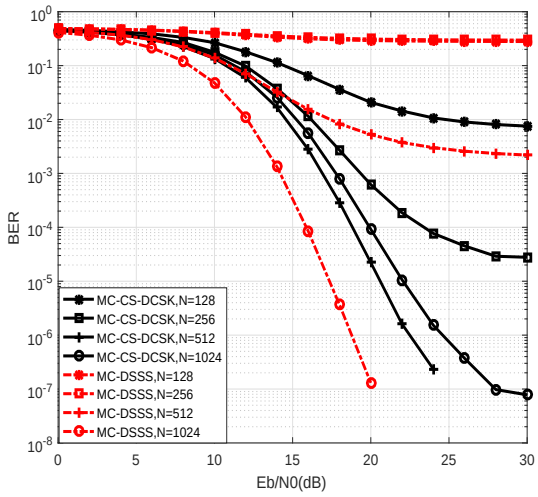

(a) BER performance

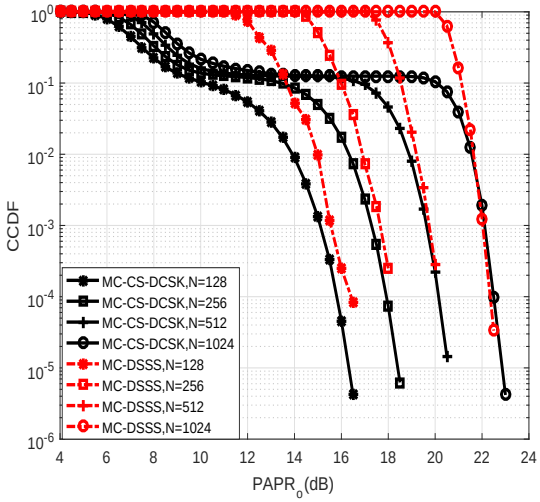

(b) PAPR performance

Fig. 7: Comparisons of BER and PAPR performance between MC-CS-DCSK and MC-DSSS over UWA channel-I. The parameters are $SF = 32, N = [128, 256, 512, 1024], CP = T_s/8$.

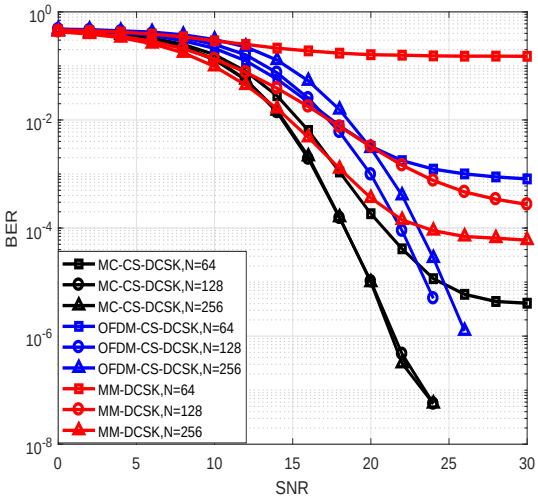

(a) UWA channel-II

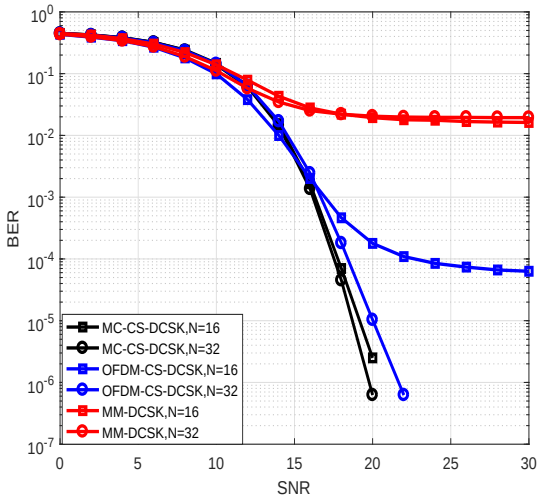

(b) UWA channel-III

Fig. 8: Comparisons of BER performance between MC-CS-DCSK, OFDM-CS-DCSK and MM-DCSK over different UWA channels. The parameters are $SF = 32, N = [16, 32, 64, 128, 256], CP = T_s/8$.

with interleaver has better than that of the system without interleaver. For example, the BER level of the system without interleaver is only reduced to 10^{-3} when $SNR = 26$dB with $N = 512$. Therefore, we can conclude that the independence among the chips can be enhanced by interleaving, which makes the system have good robustness in the UWA channels.

Since the proposed scheme is based on the non-coherent receiver without channel estimation and equalization, it is suitable for the underwater acoustic communication scenario where the channel is difficult to trace and estimate due to a time-varying characteristic.

5 Conclusion

In this paper, a novel multi-carrier chaotic spread-spectrum communication system is proposed. This system combines CS-DCSK with OFDM so that the reference and the information bearing chips of CS-DCSK are transmitted in the same time/frequency unit, which makes the transmitted signal have both good anti-time/frequency-selective fading capacity. Simulation results over UWA channels show that the proposed system has better performance than MC-DSSS, MM-DCSK, and OFDM-CS-DCSK. Analytical BER expressions have been derived under AWGN channels and multipath Rayleigh channels, the correctness has been validated by simulation.

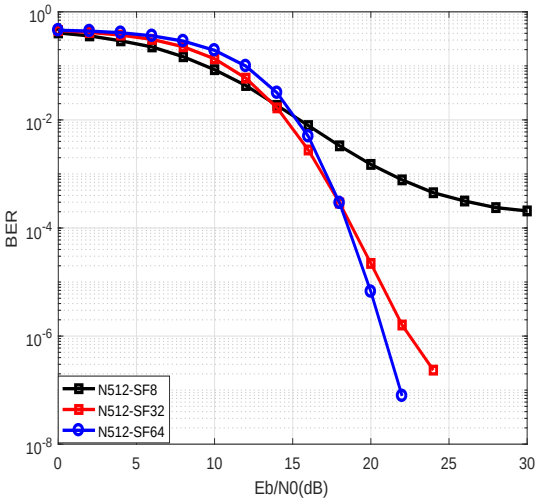

(a) UWA channel-I

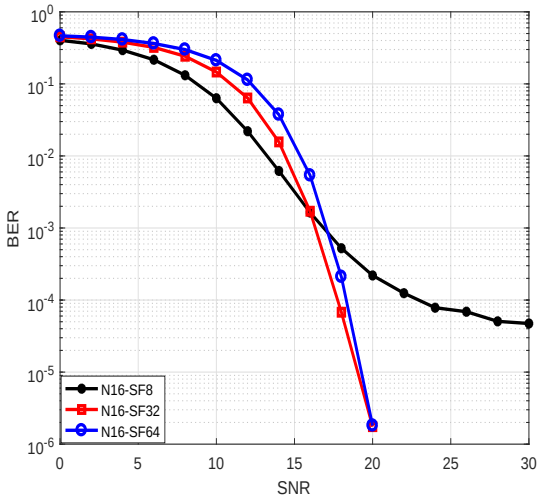

(b) UWA channel-III

Fig. 9: The effect of spreading factors on BER performance over UWA channel-I and UWA channel-III. The parameters are $SF = [8, 32, 64], N = [16, 512], CP = T_s/8$.

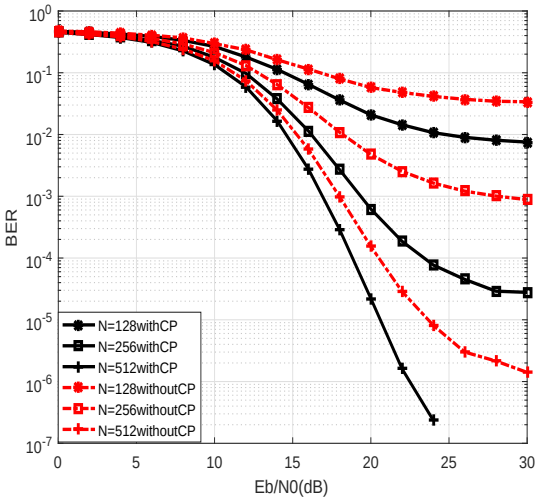

(a) The effect of CP

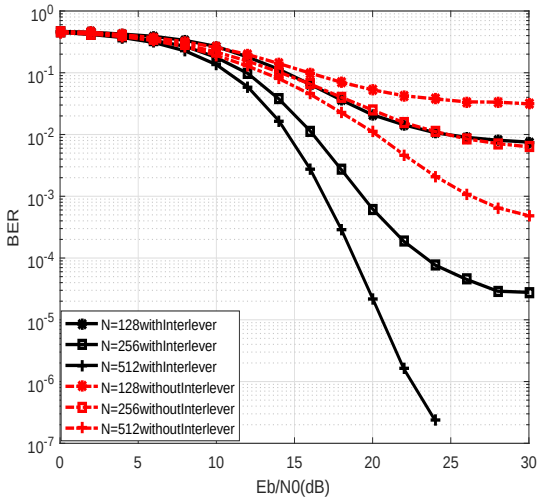

(b) The effect of interleaver

Fig. 10: The effect of CP and interleaver on BER performance over UWA channel-I. The parameters are $SF = 32, N = [128, 256, 512]$.

6 References

1 Zhou G., Li Y., He Y. C., et al.: 'Artificial fish swarm based power allocation algorithm for MIMO-OFDM relay underwater acoustic communication', *IET Communications,* 2018, **12**, (9), pp. 1079-1085

2 Diamant R., Lampe L.: 'Low probability of detection for underwater acoustic communication: A review', *IEEE Access,* 2018, **6**, pp. 19099-19112

3 Qu F., Qin X., Yang L., Yang T. C.:'Spread-spectrum method using multiple sequences for underwater acoustic communications', *IEEE J. Ocean. Eng.,* 2017, DOI: 10.1109/JOE.2017.2750298

4 Xu L. J., Zhong X., Yu H., et al.: 'Spatial and time-reversal diversity aided least-symbol-error-rate turbo receiver for underwater acoustic communications', *IEEE Access,* 2018, **6**, pp. 9049-9058

5 Marchetti L., Reggiannini R.: 'An efficient receiver structure for sweep-spread-carrier underwater acoustic links', *IEEE J. Ocean. Eng.,* 2015, **41**, (2), pp. 440-449

6 Gorokhov A., Linnartz J. P.:'Robust OFDM receivers for dispersive time-varying channels: equalization and channel acquisition', *IEEE Trans. Wireless Commun.,* 2004,**52**, (4), pp. 572-583

7 Radosevic A., Ahmed R., Duman T. M., et al.:'Adaptive OFDM modulation for underwater acoustic communications: design considerations and experimental results', *IEEE J. Ocean. Eng.,* 2014,**39**, (2), pp. 357-370

8 Suzuki T., Wada T., Yamada H., et al.:'A 31.8kbps/8kHz underwater acoustic single carrier frequency division multiplexing (SC-FDM) communication system with forward error correction', *IEEE OCEANS-Anchorage,* AK, USA, Dec. 2017, pp. 1-5

9 Mostofi Y., Cox D. C.:'ICI mitigation for pilot-aided OFDM mobile systems', *IEEE Trans. Wireless Commun.,* 2005, **4**, (2), pp. 765-774

10 Kirstem V., Molisch A. F., Christen L.: 'Jammer sensing and performance analysis of MC-CDMA ultrawideband systems in the presence of a wideband jammer', *IEEE Trans. Wireless Commun.,* 2018, DOI:10.1109/TWC.2018.2816641

11 Kondo S., Milstein B.: 'Performance of multicarrier DS CDMA systems', *IEEE Trans. Wireless Commun.,* 1996, **44**,(2), pp.238-246

12 Lok T. M., Wong T. F., Lehnert J. S.: 'Blind adaptive signal reception for MC-CDMA systems in Rayleigh fading channels', *IEEE Trans. Wireless Commun.,* 1999, **47**,(3), pp. 464-471

13 Konstantakos D. P., Adams A. E., Sharif B. S.: 'Multicarrier code division multiple access (MC-CDMA) technique for underwater acoustic communication networks using short spreading sequences', *IEE Proceedings - Radar, Sonar and Navigation,* 2004, **151**, (4), pp. 231-239

14 Li M., Liu C., Hanly S. V.: 'Precoding for the sparsely spread MC-CDMA downlink with discrete-alphabet inputs', *IEEE Trans Vehicular Technology,* 2016, **66**,(2), pp. 1116-1129

15 Ye L., Chen G., Wang L.: 'Essence and advantages of FM-DCSK technique versus traditional spreading spectrum communication method', *J. Circuits, Systems and Signal Processing*, 2005, **24**, (9). pp. 657-673

16 Kennedy M. P., Kolumbán G., Kis G., Jako Z.: 'Performance evaluation of FM-DCSK modulation in multipath environments', *IEEE Trans. Circuits Syst.-I*, 2000, **47**, (12), pp. 1702-1711

17 Escribano F. J., Kaddoum G., Wagemakers A., et al.:'Design of a new differential chaos-shift-keying system for continuous mobility', *IEEE Trans. Wireless Commun.,* 2016, **65**, (5), pp. 2066-2078

18 Galias Z., Maggio G. M.:'Quadrature chaos-shift keying: Theory and performance analysis', *IEEE Trans. Circuits Syst.-I, Fundam. Theory Appl,* 2001, **48**, (12), pp. 1510-1519

19 Wang L., Cai G., Chen G.: 'Design and performance analysis of a new multiresolution M-ary differential chaos shift keying communication system', *IEEE Trans. Wireless Commun.*, 2015, **14**, (9), pp. 5197-5208

20 Xu W. K., Wang L., Kolumbán G.: 'A new data rate adaption communications scheme for code-shifted differential chaos shift keying modulation', *Int. J. Bifur. Chaos,* 2012,**22**, (8), pp. 1-8

21 Kaddoum G.: 'Design and performance analysis of a multi-user OFDM based differential chaos shift keying communication system', *IEEE Trans. Commun.*, 2016, **64**, (1), pp. 249-260

22 Kaddoum G., Richardson F. D., Gagnon F.:'Design and analysis of a multi-carrier differential chaos shift keying communication system', *IEEE Trans. Commun.*, 2013, **61**, (8), pp. 3281-3291

23 Huang T., Wang L., Xu W., Chen G.: 'A multi-carrier M-ary differential chaos shift keying system with low PAPR', *IEEE Access,* 2017, **5**, pp. 18793-18803

24 Yang H., Tang Wallace, K. S., Chen G., Jiang G.-P.: 'Multi-carrier chaos shift keying: system design and performance analysis', *IEEE Trans. Cir. Syst.-I*, 2017, **64**, (8), pp. 2182-2194

25 Chen M., Xu W., Wang D., Wang L.: 'Design of a multi-carrier different chaos shift keying communication system in doubly selective fading channels', *2017 23rd Asia-Pacific Conference on Communications (APCC)*, Perth, Australia, Dec. 2017, pp.1-6

26 G. Kolumbán, G. Kis.: 'Multipath performance of FM-DCSK chaos communications system', *in Proc. 2000 International Symposium on Circuits and Systems*, Geneva, Switzerland, May, 2000, pp.433-436

27 Y. Xia, C. K. Tse, F. C. M. Lau.: 'Performance of differential chaos shift keying digital communication systems over a multipath fading channel with delay spread', *IEEE Trans. Circuits and Systems II.*, 2004, **51**, pp.680-684

28 F. Lau, C. Tse.: 'Chaos-based digital communication systems', *Springer-Verlag*, 2003

29 M. Sushchik, L. S. Tsimring, A. R. Volkovskii.: 'Performance analysis of correlation-based communication schemes utilizing chaos', *IEEE Trans. Circuits and Systems I.*, 2000, **47**, pp.1684-1691

30 Xing S. Y., Gang Q., Lu M.:'A blind side unformation detection method for partial transmitted sequence peak-to-average power reduction scheme in OFDM underwater acoustic communication system', *IEEE Access,* 2018, **6**, pp. 24128-24136

31 Qarabaqi P., Stojanovic M.:'Statistical characterization and computationally efficient modeling of a class of underwater acoustic communication channels', *IEEE J. Ocean. Eng.,* 2013, **38**, (4), pp. 701-717